The complex of hypericin with β-lactoglobulin has antimicrobial activity with perspective applications in dairy industry

The complex of hypericin with β-lactoglobulin has antimicrobial activity with perspective applications in dairy industry

Beatriz Rodríguez-Amigo,[*] Pietro Delcanale,[†] Gabriel Rotger,[*] Jordi Juárez-Jiménez,[‡] Stefania Abbruzzetti,[†] Andrea Summer,[§] Montserrat Agut,[*] F. Javier Luque[‡], Santi Nonell[*] and Cristiano Viappiani[†]

[*] *Institut Quimic de Sarrià, Universitat Ramon Llull, Via Augusta 390, 08017 Barcelona, Spain;*

[†]*Dipartimento di Fisica e Scienze della Terra, Università di Parma, Viale delle Scienze 7A, 43100, Parma, Italy.*

[‡] *Departament de Fisicoquímica and Institut de Biomedicina, Facultat de Farmàcia, Universitat de Barcelona, Avda. Prat de la Riba 171, 08921 Santa Coloma de Gramenet, Spain.*

[§] *Dipartimento di Scienze degli Alimenti, Università di Parma, via del Taglio, 10, 43126 Parma, Parma, Italy.*

Corresponding author: C. Viappiani. E-mail: cristiano.viappiani@fis.unipr.it

Running head: Bactericidal action of hypericin-β-lactoglobulin

Interpretative summary

The naturally-occurring pharmacologically active hypericin compound forms a stable complex with the dimeric form of β-lactoglobulin (β–LG). The complex exhibits fluorescence and singlet oxygen photosensitizing properties. It is active against *Staphylococcus aureus* bacteria. Overall, the results are encouraging for pursuing the potential application of the complex between hypericin and β–LG as a nanodevice with bactericidal properties.

ABSTRACT

Using a combination of molecular modelling and spectroscopic experiments, the naturally-occurring pharmacologically active hypericin compound is shown to form a stable complex with the dimeric form of beta-lactoglobulin (β−LG). Binding is predicted to occur at the narrowest cleft found at the interface between monomers in the dimeric β−LG. The complex is able to preserve the fluorescence and singlet oxygen photosensitizing properties of the dye. The equilibrium constant for Hyp binding has been determined as K_a = 1.40±0.07 μM^{-1}, equivalent to a dissociation constant K_d = 0.71±0.03 μM. The complex is active against *Staphylococcus aureus* bacteria. Overall, the results are encouraging for pursuing the potential application of the complex between hypericin and β–LG as a nanodevice with bactericidal properties for disinfection.

Key words: Hypericin, β-lactoglobulin, photosensitizer, antimicrobial

INTRODUCTION

Antimicrobial products are important for the health and welfare of livestock, but a prudent use is necessary. In fact, the overuse of antibiotics can generate drug-resistant bacteria, with their possible transfer to the food chain (Guide to Prudent Use of Antimicrobial Agents in Dairy Production, 2013). For example, methicillin-resistant *Staphylococcus aureus* (MRSA) is a well-known foodborne pathogen that produces heat-stable enterotoxins during growth on a variety of foods, and is an important regional cause of human infection. (Doyle et al., 2011) Recently, it has been evidenced that livestock animals can be reservoirs of MRSA, and transmit it to humans that live in close contact with them. MRSA from animals is named Livestock Associated-MRSA (LA-MRSA) (Graveland et al., 2011). For this reason, it is important to develop new alternative strategies for preventing and treating infectious animal diseases of bacterial origin (Trevisi et al., 2014). Indeed, development of novel methods for decontamination of food-processing and handling environment is a key topic for food science. (Demirci and Ngadi, 2012, Kairyte et al., 2012, Luksiene and Brovko, 2013)

Antibacterial photosensitization-based treatment (APBT) is an emerging methodology that relies on the combined action of an otherwise nontoxic molecule (called photosensitizer), visible light, and oxygen to produce cytotoxic effects by the photoinduced generation of reactive oxygen species (photodynamic effect), particularly singlet oxygen ($^1O_2$). Thus, photoexcitation of the photosensitizers leads to the formation of $^1O_2$, a non-radical, electronically-excited form of the dioxygen molecule that is highly reactive against a vast array of cellular components ranging from membrane lipids to proteins and nucleic acids. (Jori et al., 2011, Ogilby, 2010) APBT has proved to be valuable for the treatment of localized microbial infections, effectively acting on several classes of microbial pathogens, without inducing insurgence of photoresistant species even after multiple treatments. The selectivity of microbial cell killing in comparison with the constituent host tissues, and the possibility to activate photodynamic sensitizers by means of inexpensive and safe visible light sources, are further elements in favor of the methodology. (Jori et al., 2011)

Hypericin (Hyp; Figure 1) is a natural product, structurally belonging to the chemical class of naphthodianthrones, which is found in plants from the genus *Hypericum, e.g., St. John's Wort,* (Brockmann et al., 1939, Duràn and Song, 1986). St. John's Wort infusions are being used as herbal aids for depression and Hyp has also been utilized as an antiviral, (Jacobson et al., 2001, Kubin et al., 2005) antibacterial, (Kairyte et al., 2012, Yow et al., 2012), and antifungal agent. (Rezusta et al., 2012). The antimicrobial photoactivity of Hyp against MRSA, both *in vitro* and *in vivo*, has been recently assessed (Nafee et al., 2013). While Hyp is largely insoluble in water, it dissolves readily in ethanol or dimethylsulfoxide (DMSO), where it displays a bright red colour due to its absorption and fluorescence emission properties. (Duràn and Song, 1986, López-Chicón et al., 2012) In these solvents, Hyp is also a strong photosensitizer, with yields exceeding 0.7. (Fehr et al., 1995, Michaeli et al., 1993) When dissolved in water, Hyp tends to form aggregates, which results in broadening of the bands in the absorption spectrum, in a much weaker, broad and structureless fluorescence emission, and loss of singlet oxygen photosensitizing efficiency (Yamazaki et al., 1993).

Since the effectiveness of Hyp-mediated photodynamic action is heavily dependent on the specific localizing capability of the delivery methodology, proteins appear as particularly interesting delivery agents thanks to their high biocompatibility, bioavailability, and the possibility to select specific proteins suitable to the environment to be targeted. We have recently shown that Hyp binds to the hydrophobic pocket of apomyoglobin preserving its fluorescence and $^1O_2$ photosensitizing properties. (Comas-Barceló et al., 2013) Furthermore, we have shown that the complex is active against *Staphylococcus aureus* bacteria.

In this work we propose the use of β-lactoglobulin (β-LG), because it is the most abundant protein in the whey of cow's milk, (Flower et al., 2000) as a delivery vehicle for antimicrobial photodynamic application of Hyp. β-LG is a small, homodimeric protein of 162 amino acids (~18,400 Da) belonging to the lipocalin family. (Åkerström et al., 2006, Mercadante et al., 2012) Owing to their ability to bind small hydrophobic molecules, while simultaneously being recognized by cell surface receptors, lipocalins were suggested as potential systems for drug delivery. (Åkerström et al., 2006) While some

lipocalins possess high ligand specificity, others, as β-LG, demonstrate a remarkable versatility in their ligand binding patterns. Affinity for small molecules is generally intermediate, with dissociation constants (K_d) around 1 μM. In this work we have used the B variant of β-LG, characterized by glycine and alanine at positions 64 and 118, (Tanford and Nozaki, 1959) to examine the ability to bind Hyp and the effect of binding on the photodynamic properties of Hyp. Worthwhile, we show that the complex between β-LG and Hyp is able to inactivate *Staphylococcus aureus* bacteria. In view of the biocompatibility of the β-LG carrier with dairy products as well as with milk processing and handling material, this construct has potential impact for photodynamic antibacterial applications in dairy industry.

MATERIALS AND METHODS

Hyp was obtained from HWI Analytik GmbH. β-LG (isoform B) from bovine milk was obtained from Sigma Aldrich. All samples were used as received.

Docking calculations.

The protein model for the bovine β-LG dimer was derived from the X-ray crystallographic structure (PDB entry 1BEB) (Brownlow et al., 1997). The structure was refined by including addition of hydrogen atoms using the xLEAP facility in AMBER12 (Case et al., 2012) and the parm99SB (Hornak et al., 2006) force field, removal of non-standard residues (sulphate anion) and generation of the disulfide bonds Cys66-Cys160 and Cys106-Cys119. Since the N- and C-terminal segments are not observed in the X-ray structure, N-methylamine and acetyl capping groups were added to the C- and N-terminus, respectively. The binding of Hyp was explored by means of docking calculations carried out with GLIDE (Friesner et al., 2004) (Halgren et al., 2004). Since the size of Hyp preclude its binding to the cavity shaped in the interior of the lipocalin-type β-barrel, docking was performed in the two pockets formed at the interface of the monomers in the dimeric complex. The first pocket

included the solvent-exposed residues inside a cube of 39300 $Å^3$, which was centered between side chains of residues Arg148 of one monomer and Asp137 of the other. The second cavity was defined by the exposed residues inside a cube of the same size centered at the midpoint of the segment that connects the side chains of residue Trp61 in each monomer.

General spectroscopic instrumentation

Absorption spectra recorded using a Varian Cary 6000i (Varian Inc., Palo Alto, CA). Fluorescence spectra were recorded using a Spex-Fluoromax 4 (Horiba Jobin Yvon, Edison, NJ) or a Perkin Elmer LS50 spectrofluorometers.

Singlet oxygen detection

Production of the reactive species singlet oxygen was assessed by monitoring its specific phosphorescence at 1275 nm with a setup described in detail elsewhere. (Jiménez-Banzo et al., 2008) Hyp was excited by a pulsed laser at 532 nm and the emission of singlet oxygen was detected by a dedicated NIR photomultiplier.

Microbial strains and growth conditions

Staphylococcus aureus CECT 239 was obtained from the Spanish Type Culture Collection (CECT). Bacterial cells were grown overnight in sterile Tryptic Soy Broth (TSB) at 37°C. Stock inoculum suspensions were prepared in PBS and adjusted to optical densities of 0.4 at 600 nm.

Photodynamic inactivation of *S. aureus*

Cell suspensions in PBS were incubated with the photosensitizer for 30 minutes in the dark at room temperature. Then, 0.3 mL of the suspensions were placed in 96-well plates. The plates were illuminated from the top by use of LED green light for 15 or 30 minutes (18 and 37 $J \cdot cm^{-2}$, respectively), then serially diluted, seeded on Tryptic Soy-Agar and incubated for 24 h at 37°C. Experiments were carried out in duplicate for each condition, including cell controls and dark controls. Colony-forming units (CFUs) were counted in order to calculate the survival fraction.

136

137 ## RESULTS AND DISCUSSION

138 ### Modelling of β–LG-Hyp interaction

139 β-LG forms dimers (2β-LG) under conditions close to those encountered physiologically, with a
140 dimerization constant K_D = 8.6 μM at pH = 7.5. (Mercadante et al., 2012) β-LG is shaped to
141 accommodate small hydrophobic compounds, such as retinol and the aliphatic chains of fatty acids,
142 in the lipocalin-type β-barrel. However, the cavity is too narrow to accommodate Hyp, which suggests
143 that this compound should bind other pockets. In particular, inspection of the dimeric structure of
144 β–LG revealed that Hyp might bind to the clefts formed at the interface between monomers (Figure
145 2). The analysis of the best ranked poses supported the binding of Hyp to the narrow cleft, as the
146 predicted score (-7.4 kcal/mol) is ~ 2.5 kcal/mol more favourable than the binding to the wide cleft
147 (score of -4.9 kcal/mol). This finding is not unexpected keeping in mind the hydrophobicity of the
148 compound and the narrow separation between the walls of this cleft, where Hyp is largely occluded
149 from the solvent. In contrast, binding to the wide cleft leaves one of the two faces of Hyp exposed to
150 the solvent (see Figure 2).

151

152 ### Spectroscopic analysis of Hyp binding to β–LG.

153 Binding between Hyp and 2β-LG can be monitored through the effects on the absorption spectrum
154 and fluorescence emission. Aqueous solutions of Hyp show broad absorption bands and very weak
155 and structureless fluorescence emission (Figure 3A). (Miskovsky et al., 1998) When Hyp is dissolved
156 in the presence of 2β-LG, its absorption spectrum shows sharper bands instead and, most importantly,
157 the fluorescence emission increases substantially and becomes structured (Figure 3B). These facts
158 indicate that Hyp is located in a substantially less polar environment than water, as previously
159 observed with apomyoglobin and human serum albumin, (Comas-Barceló et al., 2013, Das et al.,

160 1999, Miskovsky et al., 1998) as a result of binding to the protein. These conditions are a prerequisite
161 for preservation of the singlet oxygen photosensitization via energy transfer from the Hyp triplet state.
162 A more detailed characterization of the photophysical properties of the complex is beyond the scope
163 of the present work and will be reported elsewhere.
164 Since virtually only bound Hyp molecules are fluorescent, the recorded fluorescence emission
165 intensity is proportional to the fraction of bound molecules. Accordingly, the affinity of Hyp for 2β-
166 LG can be evaluated by monitoring the fluorescence emission as a function of Hyp concentration
167 (Figure 3C). A model for the binding equilibrium Hyp + 2β-LG ⇆ 2β-LG-Hyp (Comas-Barceló et
168 al., 2013) affords an association constant K_a = 1.40±0.07 μM^{-1}, corresponding to a dissociation
169 constant K_d = 0.71±0.03 μM.
170

171 **Singlet oxygen production**

172 Production of the reactive species singlet oxygen was demonstrated by observation of its specific
173 phosphorescence at 1275 nm. Figure 4 shows the intensity of the singlet oxygen emission of Hyp and
174 of the Hyp-2β-LG complex in aqueous solutions. Consistent with the previous results. It can be
175 clearly observed that the complex has a far superior ability than free Hyp to produce singlet oxygen.

176 **Photodynamic inactivation of *S. aureus***

177 Hyp is widely used in antimicrobial photodynamic therapy due to its bactericidal and fungicidal
178 effect. (Rezusta et al., 2012, Yow et al., 2012) To assess the corresponding effects of the Hyp-2β-LG
179 complex, photodynamic inactivation tests were carried out on *S. aureus* bacteria. The results were
180 compared with those obtained for free Hyp under the same experimental conditions (Figure 5). It can
181 be clearly seen that the complex is devoid of any dark toxicity yet it is capable of eradicating bacteria
182 (5 logs) upon exposure to visible light. Although the bacterial phototoxicity of Hyp-2β-LG is not
183 much different from that of free Hyp, a major advantage of the use of the Hyp-2β-LG complex is that

it is administered to the cell suspension using a buffered aqueous solution, which is clearly more compatible with the use in a food processing environment.

CONCLUSIONS

The complex between Hyp and β-LG preserves the singlet oxygen photosensitizing properties of Hyp. The nanostructured material is effective against *S. aureus* suspensions and can decrease the bacterial load by 5 orders of magnitude (99.999%) upon exposure to visible light. The combination of the superb antimicrobial properties of natural hypericin with the full compatibility of the protein carrier with dairy industry processes suggests that it has the potential to be introduced as an effective disinfectant for food manufacturing and handling materials. Further, this APBT might find an application in the routine of milking.

ACKNOWLEDGEMENTS

Financial support for this research was obtained from the Spanish MINECO (CTQ2013-48767-C3-1-R; SAF2011-27642), Generalitat de Catalunya (2014SGR304 and 2014SGR1189; ICREA Academia) and from Ministero degli Affari Esteri, Direzione generale per la promozione del sistema Paese (Progetti di Grande Rilevanza, Italia-Argentina 2011–2013). J.J-J thanks Instituto de Salud Carlos III for FIS fellowship. The Consorci de Serveis Universitaris de Catalunya is acknowledged for computational facilities.

204 **REFERENCES**

205

206 Åkerström, B., N. Borregaard, D. R. Flower, and J. P. Salier. 2006. Lipocalins. Landes Bioscience,
207 Georgetown, USA.

208 Brockmann, H., M. N. Haschad, K. Maier, and F. Pohl. 1939. Hypericin, the photodynamically active
209 pigment from Hypericum perforatum. Naturwissenschaften 32:550.

210 Brownlow, S., J. H. M. Cabral, R. Cooper, D. R. Flower, S. J. Yewdall, I. Polikarpov, A. C. T. North,
211 and L. Sawyer. 1997. Bovine beta-lactoglobulin at 1.8 angstrom resolution - Still an enigmatic
212 lipocalin. Structure 5:481-495.

213 Case, D. A., T. A. Darden, I. T. E. Cheatham, C. L. Simmerling, J. Wang, R. E. Duke, R. Luo, R. C.
214 Walker, W. Zhang, K. M. Merz, B. Roberts, S. Hayik, A. Roitberg, G. Seabra, J. Swails, A. W. Götz,
215 I. Kolossváry, K.F.Wong, F. P. J. Vanicek, R.M.Wolf, J. Liu, X. Wu, S. R. B. T. Steinbrecher, H.
216 Gohlke, Q. Cai, X. Ye, J. Wang, M.-J. Hsieh, G.Cui, D. R. Roe, D. H. Mathews, M. G. Seetin, R.
217 Salomon-Ferrer, C. Sagui, V. Babin, T.Luchko, S. Gusarov, and A. K. P. A. Kollman. 2012.
218 AMBER12. University of California, San Francisco.

219 Comas-Barceló, J., B. Rodríguez-Amigo, S. Abbruzzetti, P. d. Rey-Puech, M. Agut, S. Nonell, and
220 C. Viappiani. 2013. A self-assembled nanostructured material with photosensitising properties. RSC
221 Advances 3:17874-17879.

222 Das, K., A. V. Smirnov, J. Wen, P. Miskovsky, and J. W. Petrich. 1999. Photophysics of Hypericin
223 and Hypocrellin A in Complex with Subcellular Components: Interactions with Human Serum
224 Albumin. Photochem.Photobiol. 69(6):633-645.

225 Demirci, A. and M. O. Ngadi. 2012. Microbial decontamination in the food industry: Novel methods
226 and applications. in Series in Food Science , Technology and Nutrition. Vol. 234. Woodhead
227 Publishing.

228 Doyle, M. E., F. A. Hartmann, and A. C. L. Wong. 2011. White Paper on Sources of Methicillin-
229 Resistant Staphylococcus aureus (MRSA) and Other Methicillin-Resistant Staphylococci:
230 Implications for Our Food Supply? FRI Food Safety Reviews.
231 Duràn, N. and P. S. Song. 1986. Hypericin and its photodynamic action. Photochem.Photobiol.
232 43(6):677 - 680.
233 Fehr, M. J., M. A. McCloskey, and J. W. Petrich. 1995. Light-induced acidification by the antiviral
234 agent hypericin. J. Am. Chem. Soc. 117:1833–1836.
235 Flower, D. R., A. C. T. North, and C. E. Sansom. 2000. The lipocalin protein family: structural and
236 sequence overview. Biochimica et Biophysica Acta (BBA) - Protein Structure and Molecular
237 Enzymology 1482:9-24.
238 Friesner, R. A., J. L. Banks, R. B. Murphy, T. A. Halgren, J. J. Klicic, D. T. Mainz, M. P. Repasky,
239 E. H. Knoll, M. Shelley, J. K. Perry, D. E. Shaw, P. Francis, and P. S. Shenkin. 2004. Glide: A New
240 Approach for Rapid, Accurate Docking and Scoring. 1. Method and Assessment of Docking
241 Accuracy. J. Med. Chem. 47(7):1739-1749.
242 Graveland, H., B. Duim, E. vanDuijkeren, D. Heederik, and J. A. Wagenaar. 2011. Livestock-
243 associated methicillin-resistant Staphylococcus aureus in animals and humans. International Journal
244 of Medical Microbiology 301(630– 634).
245 Guide to Prudent Use of Antimicrobial Agents in Dairy Production. 2013. Federation Internationale
246 du Lait - International Dairy Federation.
247 Halgren, T. A., R. B. Murphy, R. A. Friesner, H. S. Beard, L. L. Frye, W. T. Pollard, and J. L. Banks.
248 2004. Glide: A New Approach for Rapid, Accurate Docking and Scoring. 2. Enrichment Factors in
249 Database Screening. J. Med. Chem. 47(7):1750-1759.
250 Hornak, V., R. Abel, A. Okur, B. Strockbine, A. Roitberg, and e. al. 2006. Comparison of multiple
251 Amber force fields and development of improved protein backbone parameters. Proteins 65:712-725.
252 Jacobson, J. M., L. Feinman, L. Liebes, N. Ostrow, V. Koslowski, A. Tobia, B. E. Cabana, D. H.
253 Lee, J. Spritzler, and A. M. Prince. 2001. Pharmacokinetics, Safety, and Antiviral Effects of

Hypericin, a Derivative of St. John's Wort Plant, in Patients with Chronic Hepatitis C Virus Infection. Antimicrobial Agents and Chemotherapy 45:517–524.

Jiménez-Banzo, A., X. Ragàs, P. Kapusta, and S. Nonell. 2008. Time-resolved methods in biophysics. 7. Photon counting vs. analog time-resolved singlet oxygen phosphorescence detection. Photochem. Photobiol. Sci. 7:1003 - 1010.

Jori, G., M. Camerin, M. Soncin, L. Guidolin, and O. Coppellotti. 2011. Chapter 1 Antimicrobial Photodynamic Therapy: Basic Principles. Pages 1-18 in Photodynamic Inactivation of Microbial Pathogens: Medical and Environmental Applications. Vol. 11. The Royal Society of Chemistry.

Kairyte, K., S. Lapinskas, V. Gudelis, and Z. Luksiene. 2012. Effective inactivation of food pathogens Listeria monocytogenes and Salmonella enterica by combined treatment of hypericin-based photosensitization and high power pulsed light. J Appl Microbiol 112:1144–1151.

Kubin, A., F. Wierrani, U. Burner, G. Alth, and W. Grünberger. 2005. Hypericin-The facts about a controversial agent. Curr. Pharm. Des. 11:233–253.

López-Chicón, P., M. P. Paz-Cristobal, A. Rezusta, C. Aspiroz, M. Royo-Cañas, E. Andres-Ciriano, Y. Gilaberte, M. Agut, and S. Nonell. 2012. On the mechanism of Candida spp. photoinactivation by hypericin. Photochem. Photobiol. Sci. 11:1099-1107.

Luksiene, Z. and L. Brovko. 2013. Antibacterial Photosensitization-Based Treatment for Food Safety. Food Engineering Reviews 5(4):185-199.

Mercadante, D., L. D. Melton, G. E. Norris, T. S. Loo, M. A. K. Williams, R. C. J. Dobson, and G. B. Jameson. 2012. Bovine β-Lactoglobulin Is Dimeric Under Imitative Physiological Conditions: Dissociation Equilibrium and Rate Constants over the pH Range of 2.5-7.5. Biophys. J. 103(2):303-312.

Michaeli, A., A. Regev, Y. Mazur, J. Feitelson, and H. Levanon. 1993. Triplet state reactions of hypericin. Time-resolved laser photolysis and electron paramagnetic resonance spectroscopy. J. Phys. Chem. 97:9154-9160.

279 Miskovsky, P., D. Jancura, S. Sanchez-Cortez, E. Kocisova, and L. Chinsky. 1998. Antiretrovirally
280 Active Drug Hypericin Binds the IIA Subdomain of Human Serum Albumin: a Resonance Raman
281 and Surface-Enhanced Raman Spectroscopy Study. J. Am. Chem. Soc. 120(25):6374-6379.
282 Nafee, N., A. Youssef, H. El-Gowelli, H. Asem, and S. Kandil. 2013. Antibiotic-free
283 nanotherapeutics: Hypericin nanoparticles thereof for improved in vitro and in vivo antimicrobial
284 photodynamic therapy and wound healing. International Journal of Pharmaceutics 454(1):249-258.
285 Ogilby, P. R. 2010. Singlet oxygen: there is indeed something new under the sun. Chemical Society
286 Reviews 39(8):3181-3209.
287 Rezusta, A., P. López-Chicón, M. P. Paz-Cristobal, M. Alemany-Ribes, D. Royo-Díez, M. Agut, C.
288 Semino, S. Nonell, M. J. Revillo, C. Aspiroz, and Y. Gilaberte. 2012. In Vitro Fungicidal
289 Photodynamic Effect of Hypericin on Candida Species. Photochem.Photobiol. 88(3):613-619.
290 Tanford, C. and Y. Nozaki. 1959. Physico-Chemical Comparison of β-Lactoglobulins A and B. J.
291 Biol. Chem. 234(11):2874-2877.
292 Trevisi, E., A. Zecconi, S. Cogrossi, E. Razzuoli, P. Grossi, and M. Amadori. 2014. Strategies for
293 reduced antibiotic usage in dairy cattle farms. Research in Veterinary Science 96(229–233).
294 Yamazaki, T., N. Ohta, I. Yamazaki, and P. S. Song. 1993. Excited-state properties of hypericin:
295 electronic spectra and fluorescence decay kinetics. J. Phys. Chem. 97(30):7870-7875.
296 Yow, C. M. N., H. M. Tang, E. S. M. Chu, and Z. Huang. 2012. Hypericin-mediated Photodynamic
297 Antimicrobial Effect on Clinically Isolated Pathogens†. Photochem.Photobiol. 88(3):626-632.
298
299
300

Figure captions

Figure 1. Chemical structure of Hypericin

Figure 2. Best poses of Hyp bound to the narrow and wide clefts obtained from docking calculations. Hyp is shown as sticks (orange and blue in the forms bound to the narrow and wide clefts, respectively). The backbone of the dimeric species of β–LG is shown in green, and the grey area displays the surface of the dimer.

Figure 3. Absorption (**A**) and fluorescence emission (**B**) spectra of Hyp solutions (7 μM) in DMSO (solid green), in PBS (dotted black) and in PBS in the presence of 100 μM β-LG (dashed red). **C**. Fluorescence emission intensity (estimated from the integrated area) as a function of Hyp concentration at [β-LG] = 100 μM (circles). Assuming K_D = 8.6 μM^{-1}, this corresponds to [2β-LG] ≈ 40 μM. The solid lines are the result of the fit with a model for a single binding site for Hyp on 2β-LG (Comas-Barceló et al., 2013) and afford an association constant K_a = 1.40±0.07 μM^{-1}, corresponding to a dissociation constant K_d = 0.71±0.03 μM.

Figure 4. Production of singlet oxygen by Hyp and the complex Hyp-2β-LG in PBS. Concentrations: Hyp (8 μM) and β-LG (40 μM).

Figure 5. Light dose effects on *S. aureus* photoinactivation by the complex Hyp-2β-LG for Hyp (8 μM) and β-LG (40 μM).

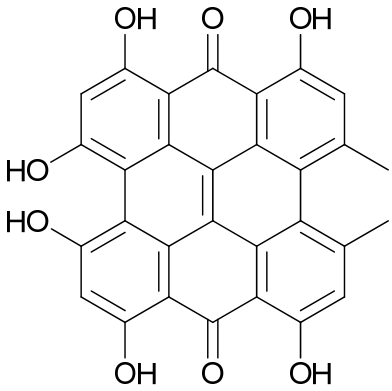

Figure 1. Rodríguez-Amigo *et al*.

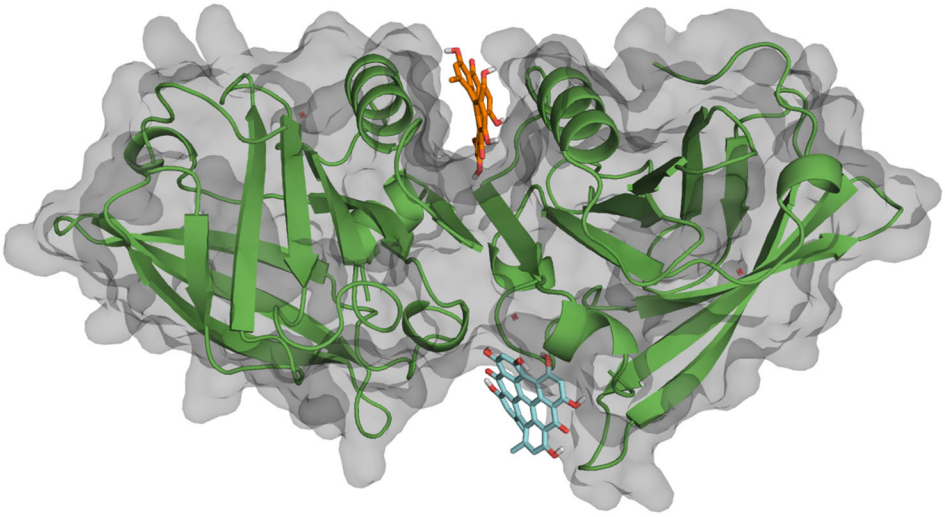

Figure 2. Rodríguez-Amigo *et al*.

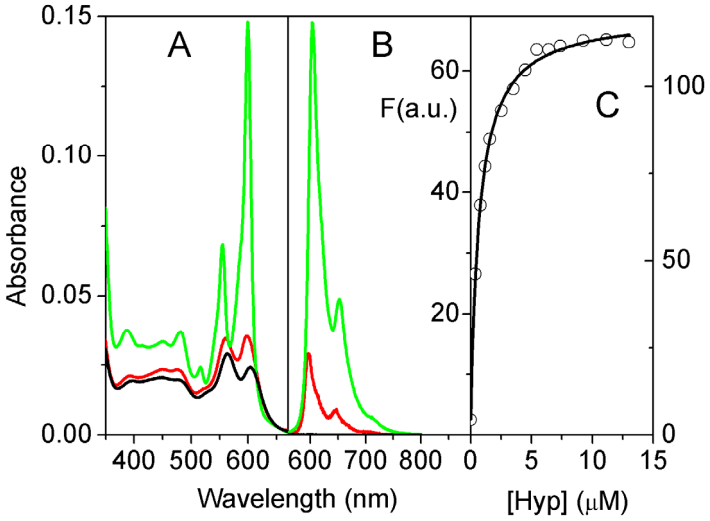

Figure 3. Rodríguez-Amigo *et al*.

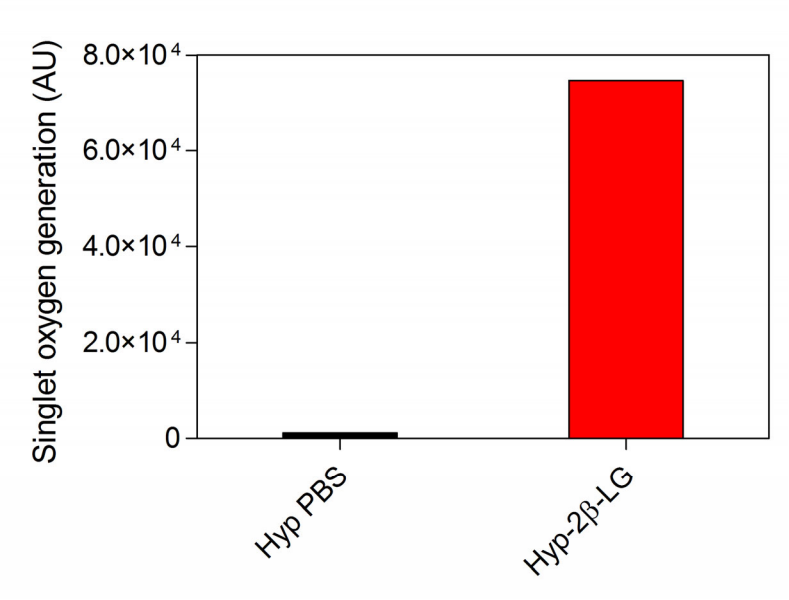

337

338

339 **Figure 4.** Rodríguez-Amigo *et al*.

340

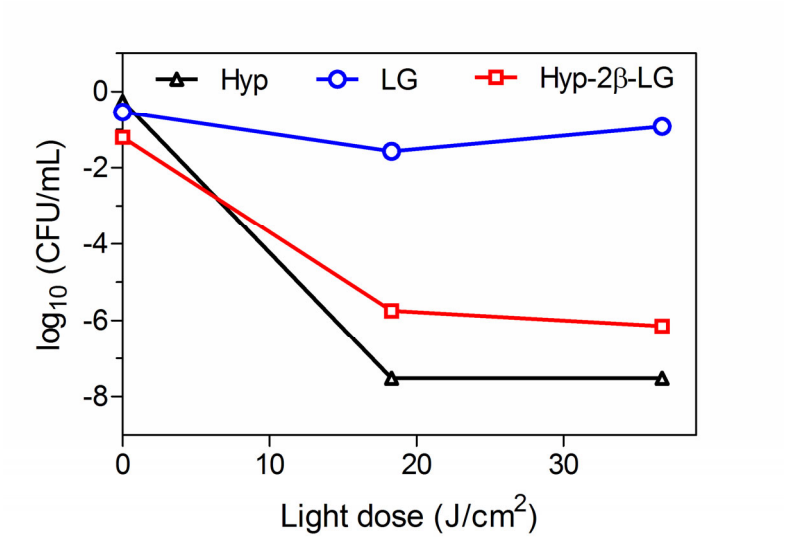

341

342

343 **Figure 5.** Rodríguez-Amigo *et al*.

344

345